AIAA JOURNAL
Vol. 37, No. 4, April 1999

Shock Oscillations in Diffuser Modeled by a Selective Noise Amplification

J.-C. Robinet* and G. Casalis†
ONERA-CERT, 31055 Toulouse CEDEX 4, France

Shock waves in supersonic flow oscillate under certain conditions. These oscillations usually have negative effects, especially for flow past transonic airfoils and in supersonic diffusers. It is therefore of practical importance to understand the origin and the consequences of these oscillations. The purpose of this paper is to model and to predict some physical characteristics of self-sustained shock oscillations in transonic diffuser flows. This paper first gives the results of a quasi-one-dimensional stability analysis. The mean flow is calculated with a code solving the averaged Navier–Stokes equations. The present stability approach however is limited to the core region where the viscous effects can be neglected. To validate the present approach, the results are compared with the experimental data of Sajben et al. (Sajben, M., Bogar, T. J., and Kroutil, J. C., "Characteristic Frequency and Length Scales in Transonic Diffuser Flow Oscillations," AIAA Paper 81-1291, June 1981) and those numerically obtained by Hsieh and Coakley (Hsieh, T., and Coakley, T. J., "Downstream Boundary Effects on the Frequency of Self-Excited Oscillations in Diffuser Flows," AIAA Paper 87-0161, Jan. 1987). As demonstrated here, the main characteristics of the oscillation are clearly obtained, for example, the shock motion spectra is reproduced correctly by the present stability approach.

Nomenclature

a	= sound velocity
h	= throat height
k	= wave number
l	= diffuser length (from throat to exit)
R_p	= exit pressure to total inlet pressure ratio
T	= temperature
t	= time
U, u	= streamwise velocity component
V, v	= transverse velocity component
X	= amplitude of shock motion
ρ	= density
$\omega/2\pi$	= frequency

Subscripts

c	= shock value
e	= exit value
f	= fluctuation value
0	= upstream value
1	= downstream value

Superscripts

$\bar{}$	= mean value
$\tilde{}$	= amplitude function for the perturbation

I. Introduction

UNDER certain conditions the shock wave in supersonic flows may exhibit oscillations, which occur, for example, with transonic airfoils and in supersonic diffusers. Different approaches have been used to quantify these oscillations and to understand their physical origin. Many experiments have been carried out by Sajben et al.[1] in the beginning of the 1980s, whereas some numerical simulations have been tried by Liou et al.[2] and Hsieh and Coakley.[3] A new approach that is more theoretical than the two others and that can thereby provide a new insight into this difficult problem is proposed in this paper. The geometry of the diffuser, the shock intensity, the separation bubble of the boundary layer just downstream of the shock, and the subsonic core region play an important role in these oscillations. But neither the experiment nor the numerical simulations can explain who does what, how, and why. The objective is to prove by simple models that the frequency of the self-sustained oscillations at least can be predicted by a small perturbation technique based on inviscid perturbations superimposed to a viscous mean flow.

The first part describes the published results: the experimental and the numerical ones. In the second part the theoretical aspects of a quasi-one-dimensional stability analysis are described. This approach consists in studying these oscillations using a simple linear stability analysis. This analysis is restricted to the core region where the viscous effects are negligible, and, in accordance with experimental results, the mean flow is assumed to be nearly one-dimensional in this region. However, the mean flow is calculated using the code FLU3M developed at ONERA to obtain accurate values for the mean flow. The one-dimensional stability results are then presented in comparison with Sajben's experiments and with the Hsieh numerical simulations. The results are finally compared both to experimental results and to the results provided by the previous simplified stability approach.

II. Background of the Present Study

Diffuser Geometry

The major experimental contribution on self-sustained shock oscillations has been brought by the McDonnell Douglas team headed by M. Sajben.[1,4,5] One of the diffusers used in the experiment is asymmetric with a flat bottom wall and a converging–diverging channel with a maximum 9-deg divergence angle. This diffuser is equipped with many suction slots, so that the flow can be considered two-dimensional at least in the middle section between the two lateral walls of the channel. Figure 1 gives a sketch of the experimental setup.

The relative diffuser length is l/h where h is the height at the throat; the length origin is chosen at the throat. In this paper only the diffuser lengths such as $l/h \leq 13$ are studied with the proposed approaches.

General Descriptions

In this nozzle the fluid accelerates from subsonic to supersonic speed through a sonic throat and is abruptly decelerated by a shock wave located downstream of the throat. The flow in this diffuser is exhausted directly to the ambient air, so that the boundary conditions at the exit cross section are closely characterized by a spatially

Received May 7, 1998; revision received Nov. 23, 1998; accepted for publication Nov. 25, 1998.

*Ph.D. Student, Aerodynamics and Energetics Modeling Department, 2, avenue Edouard Belin, B.P. 4025. E-mail: jcrobine@onecert.fr.

†Scientist Engineer, Aerodynamics and Energetics Modeling Department.

and temporally constant static pressure. The flow conditions then are characterized mainly by the ratio of the static pressure at the exit section to the total pressure at the inlet: $R_p = p_e/p_t$. This ratio determines, among other properties, the shock strength and the Mach number M_0 ahead of the shock. The flow patterns obtained with this diffuser depend on the Mach number. In Sajben's experiment shock-induced separation occurs for Mach numbers M_0 greater than 1.3, and, in this case, spontaneous self-oscillations have been observed. These oscillations consist of a shock oscillating motion together with the occurrence of fluctuations downstream of the shock. In all cases no oscillation has been observed in the supersonic zone. The following results are limited to one value of R_p: $R_p = 0.72$ ($M_0 = 1.34$).

Experimental and Numerical Results

Among Sajben's experimental results the shock motion power spectrum is of particular interest. This spectrum[4] is represented in Fig. 2, which shows that the most sensitive frequencies, for a diffuser length $l/h = 14.4$, are close to 200 Hz. Different lengths ($12 \le l/h \le 30.5$) have been studied by Sajben et al.[1] Computations have been performed by Hsieh and Coakley[3] and Liou and Coakley[6] for the same diffuser configuration. These simulations consisted in solving the unsteady averaged Navier–Stokes equations with a classical turbulence model. They were achieved in two steps: steady computations provided the mean flow, and then the unsteady computations determined the fluctuating quantities. These unsteady computations have been realized by imposing a fluctuating pressure at the exit section. Hsieh and Coakley[3] used different diffuser lengths (Table 1). Figure 3 shows the computed shock motion power spectrum corresponding to these cases. When the diffuser length l/h is less than 12, the frequency of oscillation reduces from 300 to 210 Hz as the downstream boundary location varies from $l/h = 8.6$ to 12.08, whereas the frequency increases to 310 Hz for the greatest length ($l/h = 14.7$). The latter does not agree with the experimental result (198 Hz) published by Sajben et al.[1] and given in Fig. 2.

Table 1 Oscillation frequency for different diffuser lengths (numerical results)

Frequency, Hz	l/h (case)
300	8.66 (A)
250	10.06 (B)
210	12.08 (C)
310	14.7 (D)

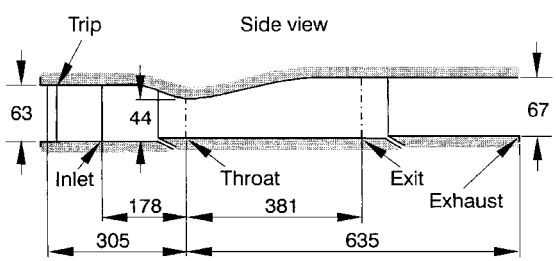

Fig. 1 Sajben et al.[1] diffuser model.

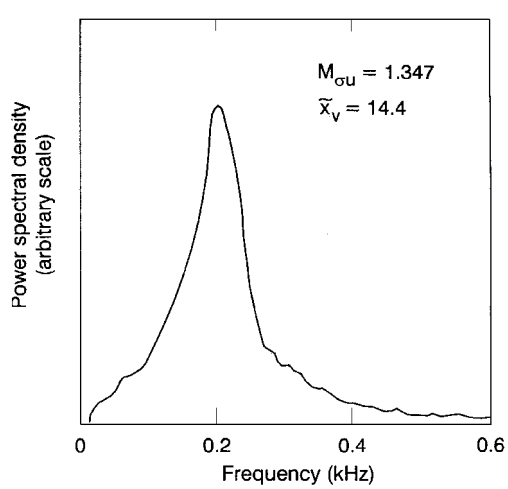

Fig. 2 Shock motion power spectrum: experiment.

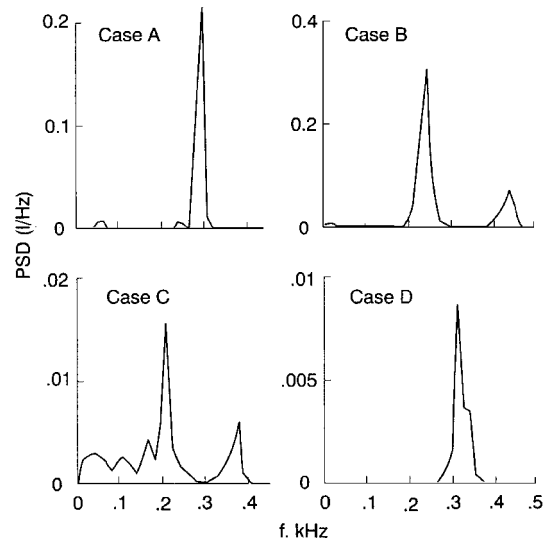

Fig. 3 Shock motion power spectrum: computation.

Taking into account all of the published results (experiment and numerical simulations), the present analysis is devoted to a simpler and more analytical approach. Let us summarize, the different diffuser lengths used in Sajben's experiment, in Hsieh's calculation, and in our present approach: Sajben's experiment, $12 \le l/h \le 30.5$; Hsieh's simulation, $8.6 \le l/h \le 14.7$; and the present approach, $8.6 \le l/h \le 13$.

The upper limit of l/h used in our approach ($l/h \le 13$) comes from the available mean flow computation performed in ONERA.[7]

III. Mean and Fluctuating Flows

The purpose of this section is to describe the main assumptions employed in the proposed small perturbation technique. The classical coordinate system (x, y) is used, where x is the streamwise coordinate and y is perpendicular to it.

Small Perturbation Technique

The two present approaches are based on the standard small perturbation technique. The instantaneous flow is written as the superposition of a basic flow and of a small fluctuation. All physical quantities q (velocity, pressure, . . .) are thus decomposed into a mean value and a fluctuating one:

$$q = \bar{q} + q_f \tag{1}$$

The physical quantities related to the mean flow are overlined, for example, $\bar{U}$ is the mean streamwise velocity component.

Mean Flow Calculation

The mean flow comes from a computation. The code FLU3M[8] developed at ONERA solves the average Navier–Stokes equations; a Jones–Launder k–ε model has been used. This computation is similar in principle to the first step of the numerical simulation done by Liou and Coakley.[6] This model allows a good representation of the shock-boundary layer interaction.[9] Before describing the formalism of the proposed model, we must first check that the computed mean flow is in agreement with Sajben's experimental results.

The two different grids have been used for the computation of the mean flow. The first one consists of a 136×99 grid with a fine distribution of points only near the upper and lower walls in order to have enough points in the boundary layers. In the x direction the mesh is strengthened around the expected shock wave location. The second computational grid (136×111 points) is refined in the y direction in the central zone of the diffuser to compute the evolution

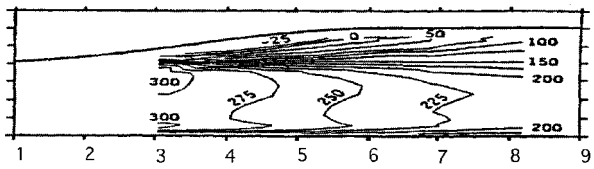

Fig. 4 $\bar{U}$ contours (m/s): experiment.

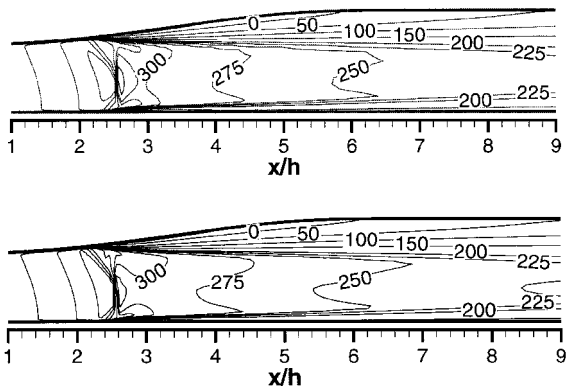

Fig. 5 $\bar{U}$ contours (m/s): computation. Top, (136 × 99) points, and bottom, (136 × 111) points.

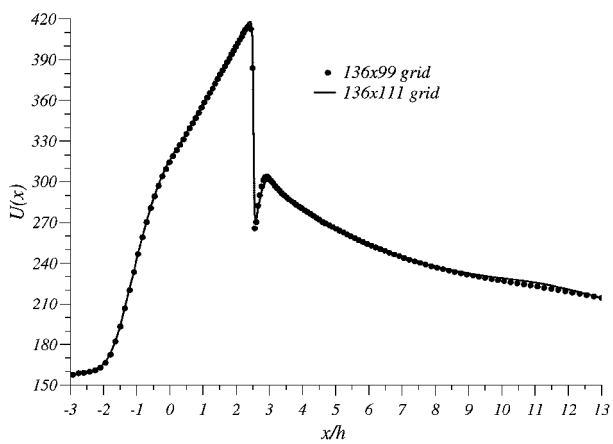

Fig. 6 Mean flow evolution: core flow.

in the y direction of mean flow more accurately. Figures 4 and 5 show the experimental and numerical results respectively for the iso-$\bar{U}$ contours. From these results it can be concluded that both computed mean flows are in good agreement with the experimental data. However, a detailed study shows that small differences still exit just downstream of the shock and between the y derivative of the different mean flow quantities.

An instructive behavior is provided by the evolution of the longitudinal mean velocity in the x direction (and in the middle of the core flow); see Fig. 6. Instead of a continuous decrease up to the exit section, the mean flow increases just downstream of the shock before decreasing. This expansion effect results from the large separation bubble in the upper boundary layer. The boundary layers' separation generates a local acceleration. This characteristic is present only in the middle of the diffuser, which is not obtained by solving the steady inviscid equations. The experimental checking of this assumption could not be made because of a lack of experimental data in this configuration (in the core of the diffuser, for $R_p = 0.72$). This local acceleration however may be the origin of the shock oscillation. For many years it has been well known that the shock is unstable in a converging nozzle, i.e., when the flow accelerates,[10] and subsequently the proposed approaches will take into account the separated region, but only through the mean flow values. So in these approaches, the boundary layer and its separated region are considered as steady.

Basic Equations for the Small Perturbation Technique

The equations for the instantaneous flow are the Euler equations, the energy equation written for the total enthalpy and the equation of perfect gas. The proposed approaches are thus limited to the core region where the viscous effects can be neglected.

Equation of continuity:

$$\frac{\partial \rho}{\partial t} + \frac{\partial(\rho U)}{\partial x} + \frac{\partial(\rho V)}{\partial y} = 0 \tag{2}$$

x-momentum equation:

$$\rho \frac{\partial U}{\partial t} + \rho U \frac{\partial U}{\partial x} + \rho V \frac{\partial U}{\partial y} + \frac{\partial P}{\partial x} = 0 \tag{3}$$

y-momentum equation:

$$\rho \frac{\partial V}{\partial t} + \rho U \frac{\partial V}{\partial x} + \rho V \frac{\partial V}{\partial y} + \frac{\partial P}{\partial y} = 0 \tag{4}$$

Enthalpy equation:

$$\rho \frac{\partial h_i}{\partial t} + \rho U \frac{\partial h_i}{\partial x} + \rho V \frac{\partial h_i}{\partial y} = \frac{\partial P}{\partial t} \tag{5}$$

Total enthalpy definition:

$$h_i = C_p T + \frac{U^2 + V^2}{2} \tag{6}$$

Equation of state:

$$P = r \rho T \tag{7}$$

where r and C_p are, respectively, the perfect gas constant ($r = 287$ $m^2 s^{-2} K^{-1}$) and specific heat coefficient ($C_p = 1007\, m^2 s^{-2} K^{-1}$).

The instantaneous flow also depends on of the Rankine–Hugoniot relations written at the instantaneous location of the shock:

$$\rho_1 (V_{n1} - W_c) = \rho_0 (V_{n0} - W_c) \tag{8}$$

$$P_1 + \rho_1 (V_{n1} - W_c)^2 = P_0 + \rho_0 (V_{n0} - W_c)^2 \tag{9}$$

$$V_{\tau 1} = V_{\tau 0} \tag{10}$$

$$C_p T_1 + \tfrac{1}{2}(V_{n1} - W_c)^2 = C_p T_0 + \tfrac{1}{2}(V_{n0} - W_c)^2 \tag{11}$$

where V_n is the velocity component normal to the shock, V_τ is the tangential component, and W_c is the velocity of the shock front.

IV. Stability Analysis

The decomposition [Eq. (1)] is first introduced into Eqs. (2–7). The mean flow, which satisfies the Navier–Stokes equations, is assumed to be a solution of the inviscid equations in this region. The resulting equations are further simplified by considering that the perturbation is small, so that the nonlinear fluctuating terms can be neglected. Finally, Eqs. (2–7) are transformed into a linear system, the coefficients of which are functions of the mean flow.

Perturbation Form

According to the experimental and numerical results, the mean flow in the core region is assumed to be weakly dependent on y, so that any mean quantity verifies the relation

$$\frac{\partial \bar{q}}{\partial y} \ll \frac{\partial \bar{q}}{\partial x}, \qquad \forall x, \forall y \tag{12}$$

With this assumption a perturbation can be sought with a uniform exponential dependence with respect to y. Thus, any fluctuating quantity is written as

$$q_f(x, y, t) = \Re \{\tilde{q}(x) \exp(\omega_i t) \exp[i(ky - \omega_r t)]\} \tag{13}$$

where $\tilde{q}$ is a complex function, k is a real wave number, and ω_i is a temporal amplification rate, whereas the real part ω_r of ω characterizes the frequency of the perturbation. $\Re(z)$ is the real part of z. The linear stability of the flow depends on the sign of ω_i: for $\omega_i < 0$ the mean flow is linearly stable, whereas for $\omega_i > 0$ the mean flow is unstable. The y dependence is justified by the fact that the mean flow is not exactly one-dimensional. There is a transverse velocity $\bar{V}$ such as $\max(\bar{U}/\bar{V}) \simeq 5.10^{-2}$. To be coherent with symmetries of the problem, the perturbation must be two dimensional ($k \neq 0$).

Stability Equations and Boundary Conditions

With the perturbation [Eq. (13)] the linearized Euler equations become an ordinary fourth-order differential system:

$$\boldsymbol{C}\frac{\mathrm{d}\boldsymbol{Z}}{\mathrm{d}x} = \boldsymbol{B}\boldsymbol{Z} \tag{14}$$

where $\boldsymbol{Z}(x)$ is the amplitude function vector of the perturbation. Its components are $\tilde{T}$, $\tilde{\rho}$, $\tilde{u}$, and $\tilde{v}$, which denote respectively the fluctuating temperature, the density, and the longitudinal and transverse velocities components. $\boldsymbol{C}$ and $\boldsymbol{B}$ are two $(4,4)$ complex matrices that are functions of the mean flow and of the coefficients ω and k.[11]

In all of the tested experimental configurations, no fluctuation has been observed in the supersonic zone flow. For this reason the first boundary condition is chosen as

$$\boldsymbol{Z}(0) = 0 \tag{15}$$

This means that there is no fluctuation at the throat. In the exit section the fluctuations do not necessarily vanish. It is imposed only that the perturbations are bounded at the exit section:

$$\|\boldsymbol{Z}(l/h)\| \ll \infty \tag{16}$$

Eigenvalue Problem

The differential system (14–16) has $\boldsymbol{Z} \equiv 0$ as a natural and trivial solution. Moreover it is the only one unless the problem becomes singular. In fact, the determinant of the matrix C is always invertible except at the position defined by $\bar{M} = 1$. The problem is thus regular from throat to shock. Then, according to the boundary condition (15), $\boldsymbol{Z} \equiv 0$ is the only solution of the problem upstream of the shock: in the whole supersonic zone there is no fluctuation. However, if the system of equations (14) is singular at the mean shock position, another solution (i.e., not trivial) may exist. To find this solution, a special procedure needs to be used at the shock position. This procedure is obtained with the shock relations (8–11).

Linearized Shock Relations

According to the small perturbation technique [Eq. (1)] and expression (13), the perturbed position of the shock is written as

$$x = \bar{x}_c + \Re\,[Xe^{i(ky-\omega t)}] \tag{17}$$

In Eq. (17), $\bar{x}_c$ represents the mean shock position ($\bar{x}_c/h \simeq 2.6$) and X the amplitude of the shock displacement that is assumed to be a small quantity. The Rankine–Hugoniot equations (8–11) are then linearized by performing a first-order Taylor expansion with respect to X. In fact, all quantities q (q_1 or q_0) are the sum of the mean and of the fluctuating values evaluated just downstream for q_1 or upstream for q_0 of the perturbed position of the shock:

$$q(x, y, t) = \bar{q}(\bar{x}_c + XE) + q_f(\bar{x}_c + XE)$$

where $E = e^{i(ky-\omega t)}$.

After expansion, q_1 is written as

$$q_1(x, y, t) = \bar{q}_1(\bar{x}_c) + \frac{\partial \bar{q}_1}{\partial x}(\bar{x}_c)XE + \tilde{q}_1(\bar{x}_c)E$$

As there is no fluctuation upstream of the shock, q_0 is simply given by

$$q_0(x, y, t) = \bar{q}_0(\bar{x}_c) + \frac{\partial \bar{q}_0}{\partial x}(\bar{x}_c)XE$$

In the preceding expression the derivative of $\bar{q}_0$ with respect to x corresponds to the left derivative (in x_0^-); the same is true with the x derivative of $\bar{q}_1$ and the right derivative (in x_0^+). After some calculation the linearized shock relations lead to an algebraic system of equations:

$$\boldsymbol{A}\boldsymbol{Z}(\bar{x}_c) = \boldsymbol{\xi}X \tag{18}$$

where $\boldsymbol{Z}(\bar{x}_c)$ is the vector of the fluctuating amplitudes calculated at $\bar{x}_c$, ξ is a complex vector, and $\boldsymbol{A}$ is a fourth-order complex matrix; A and ξ are known. From another point of view, the behavior of mean flow on both sides of shock (for example, the local convergent effect indicated in Fig. 6) occurs in the term $\boldsymbol{\xi}$ through the right and left derivatives of the mean flow. Finally, as the matrix $\boldsymbol{A}$ is invertible,[11] the vector $\boldsymbol{Z}$ at the mean shock position is known:

$$\boldsymbol{Z}(\bar{x}_c) = \boldsymbol{A}^{-1}X\boldsymbol{\xi} \tag{19}$$

All fluctuating quantities are thereby proportional to the shock oscillation amplitude X, which cannot be determined within the linear stability analysis.

Summary

The stability problem has been solved easily in the supersonic zone; $\boldsymbol{Z} = 0$ is the unique solution. In the subsonic zone the system [Eq. (14)] with the boundary conditions (15) and (16) is an eigenvalue problem. The trivial solution $\boldsymbol{Z} \equiv 0, X = 0$ is a solution. A nonzero solution can exist only if the problem is singular, which implies a particular choice of the wave number k and of the complex circular frequency ω of the perturbation. This choice corresponds to a dispersion relation between these numbers, which cannot be determined analytically. In the following a numerical procedure devoted to this point is described.

Analytical Study

If the mean flow is considered as uniform, i.e., independent of x, the differential system [Eq. (14)] becomes a linear differential system with constant coefficients. Then an analytical solution can be calculated:

$$\boldsymbol{Z}(x) = \sum_{j=1}^{4} c_j \boldsymbol{Z}_j(x) \qquad \text{with} \qquad \boldsymbol{Z}_j(x) = \boldsymbol{V}_j e^{l_j x} \tag{20}$$

where the coefficients c_j are unknown integration constants, which will be determined by the boundary conditions. l_j and $\boldsymbol{V}_j$ are respectively the eigenvalues and eigenvectors of matrix $\boldsymbol{C}^{-1}\boldsymbol{B}$ [Eq. (14)]. The expressions of l_j and $\boldsymbol{V}_j$ (Ref. 11) are given in the Appendix. Physically, the first two modes ($j = 1, 2$) correspond to the acoustic modes, respectively the downstream and upstream traveling waves, and the other two modes ($j = 3, 4$) correspond to the entropic and the rotational modes that are convected with the mean flow. To verify the condition (16), these different modes $\boldsymbol{V}_i e^{l_i x}$ cannot exhibit an exponentially increasing behavior: $\Re(l_i) \leq 0$, where $\Re(l_i)$ denotes the real part of l_i. $\Re(l_3) \leq 0$ if $\omega_i \geq 0$, $\Re(l_2) \leq 0$, and $\Re(l_1) \geq 0$ for all ω and k. Nevertheless, when $\omega_i \leq 0$, $\boldsymbol{V}_3 e^{l_3 x}$ and $\boldsymbol{V}_4 e^{l_3 x}$ are smaller than $\boldsymbol{V}_2 e^{l_2 x}$; it can then be considered that the only unacceptable mode with respect to boundary condition (16) is $\boldsymbol{V}_1 e^{l_1 x}$. The relation $c_1 = 0$ must be imposed. This relation amounts to the assumption that there are no downstream traveling waves; this is finally in agreement with Culick and Rogers's theory.[12] According to the latter, the reflected downstream traveling-wave amplitude is about six times smaller than the upstream traveling wave amplitude (in the case of the mean flow described in Sec. III). The general solution is written as

$$\boldsymbol{Z}(x) = c_2\boldsymbol{Z}_2(x) + c_3\boldsymbol{Z}_3(x) + c_4\boldsymbol{Z}_4(x) \tag{21}$$

However, according to Fig. 6, there is no evidence of the presence of any uniform zone, but, at a certain distance from the shock, it is assumed that the mean flow does not depend too much on x. In this uniform zone for $x \geq x_u$ ($x_u/h \simeq 11$), the solution of Eq. (14) can be written as Eq. (21). Equation (14) is then numerically integrated for each vector $\boldsymbol{Z}_j$ ($j = 2, 3, 4$) by decreasing values of x from the uniform zone boundary x_u up to the mean shock position $\bar{x}_c$. At this position there are two formulations of $Z(x)$: the first one comes from the numerical integration and Eq. (21), and the second one is simply given by the boundary condition (19). These two expressions

Table 2 Numerical stability results

k (m^{-1})	$\omega/2\pi = (\omega_r + i\omega_i)/2\pi$
136×99 *grid*	
−5.002	200.000 − 3.740*i*
−4.839	200.000 − 98.867*i*
136×111 *grid*	
−5.024	200.000 + 3.834*i*
−4.836	200.000 − 98.852*i*

should coincide. For a given circular frequency ω_r the unknowns are the complex constants c_2, c_3, and c_4. These six real unknowns are searched to verify the following relationship:

$$\mathbf{Z}(\bar{x}_c) = c_2\mathbf{Z}_2(\bar{x}_c) + c_3\mathbf{Z}_3(\bar{x}_c) + c_4\mathbf{Z}_4(\bar{x}_c)$$

which provides four scalar complex relations. A nonzero solution only can exist if the rank of this system of four relations is only three. This condition is a dispersion relation: it is satisfied with a particular value of (k, ω_i) for a given value of frequency $\omega_r/2\pi$ of the perturbation. A trial-and-error method finally is used to determine the eigenvalues with an initial guess for (k, ω_i) (Refs. 7 and 11). Table 2 gives the eigenvalues (k, ω_i) for the fixed frequency 200 Hz. These results have been obtained with the mean flow calculated for the diffuser length $l/h = 13$. Two modes are solutions of the stability problem. Nevertheless, only the second one, the mode (200–98.86*i*), will be considered hereafter because the first mode (200–3.74*i*) is completely dependent on the computational grid as shown in Table 2 (ω_i differs by 200%). Indeed, for this last mode the value and the sign of this ω_i strongly depend on the grid. The physical mode ($\omega_i = 200–98.8i$) is weakly dependent on x_u due to the fact that the mean flow is not strictly constant for $x_u \le x \le x_e$. More precisely, if $x_u/h \ge 11$, ω_i will only be modified by a factor of 1%. Finally, the very small obtained value of k is in agreement with the experiment and is confirmed by a full $2D$ small perturbation analysis.[13]

Computation of Shock Motion

As explained in the preceding paragraphs, the fluctuations are proportional to the shock amplitude X. To determine a spectrum from the stability results, a normalization must be introduced for the amplitude functions. As the fluctuating pressure spectrum is not known at the exit section, a uniform law is simply imposed:

$$|p_f(x_e)| = \varepsilon \bar{P}(x_e) \tag{22}$$

where ε is an arbitrary constant. The fluctuating pressure at the exit section is hence given as a fraction of the mean pressure. Finally, the shock motion spectrum is given by

$$X(\omega) = \varepsilon \frac{\bar{P}(x_e)}{\tilde{p}(x_e, \omega)} \tag{23}$$

The constant ε can be adjusted with experimental data.

Results

To validate the quasi-one-dimensional stability theory, the results are first compared with the experimental values of Sajben et al.[1] and the computations of Hsieh and Coakley.[3] The stability of the mean flow is then examined.

Shock Motion Spectra

Figure 2 shows the experimental shock motion spectrum. It exhibits a well-defined peak close to 200 Hz; this means that the shock is more sensitive to excitations of frequencies around 200 Hz. The shock motion spectrum calculated by the one-dimensional stability analysis also provides a peak close to 200 Hz. Figure 7 presents this result. This spectrum has been calculated for the $l/h = 13$ diffuser length, and the mean flow has been calculated with the 136×111 grid. To evaluate the robustness of this encouraging result, the stability analysis has been performed again but with the mean flow calculated with the 136×99 grid. Furthermore, just for the stability analysis a fine mesh in x (180 points instead of 136) has been tested

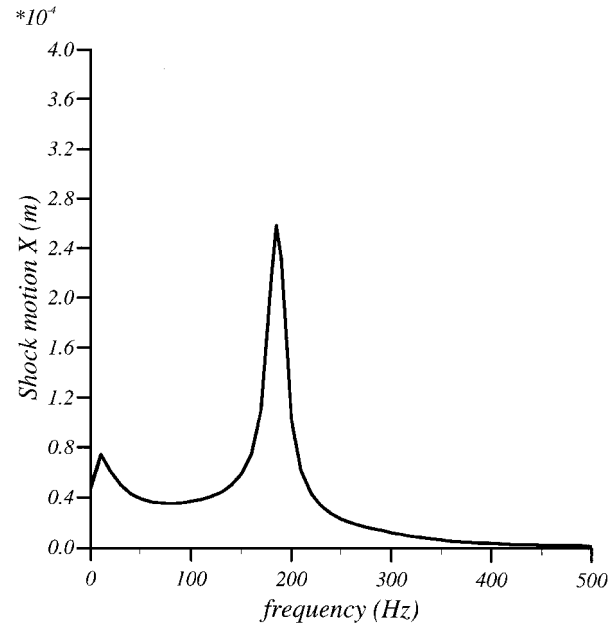

Fig. 7 Shock motion spectrum, *l*/*h* = 13.

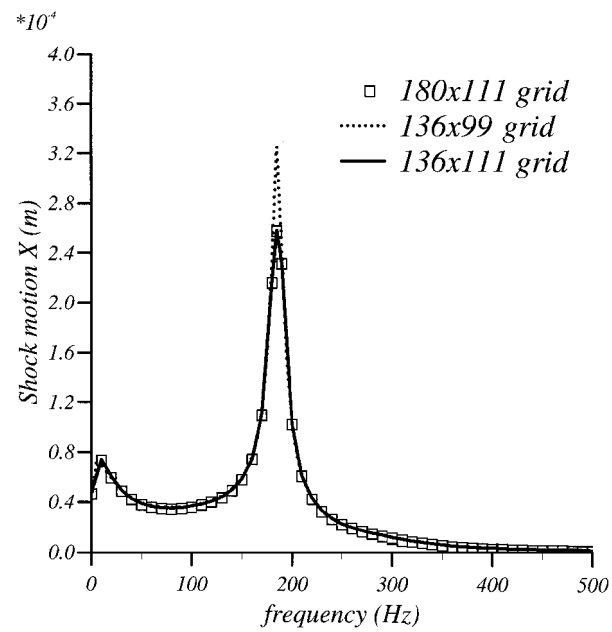

Fig. 8 Robustness of shock motion spectrum.

using a Tchebicheff polynomial interpolation for the mean flow. Figure 8 shows that the stability results do not depend either on the grid used for the stability or on the grid used for the computation of the mean flow. Concerning approximation (12), the shock motion spectra must be more or less independent of y. Figure 9 confirms this behavior where j represents the vertical index for the y line of the mesh. It seems that the quasi-one-dimensional stability theory can be applied for Sajben's experiment.

Contrary to a forced calculation or it is imposed a periodic fluctuations, often monochromatic, in the exit section, this study imposes a white noise in the exit section or no frequency is privileged. The shock responds to this white noise by selecting a very specific frequency, 200 Hz in our case. This method (the introduction of noise) is traditional when one wants to highlight the clean modes of a physical system. In our case the shock is an amplifier of noise. One fundamental parameter in the determination of the self-sustained oscillation frequency is the length of the diffuser. Different stability analyses have been performed for different lengths. Figure 10 shows the evolution of the observed frequency peak in the shock displacement spectra vs the diffuser length. For a diffuser length such as

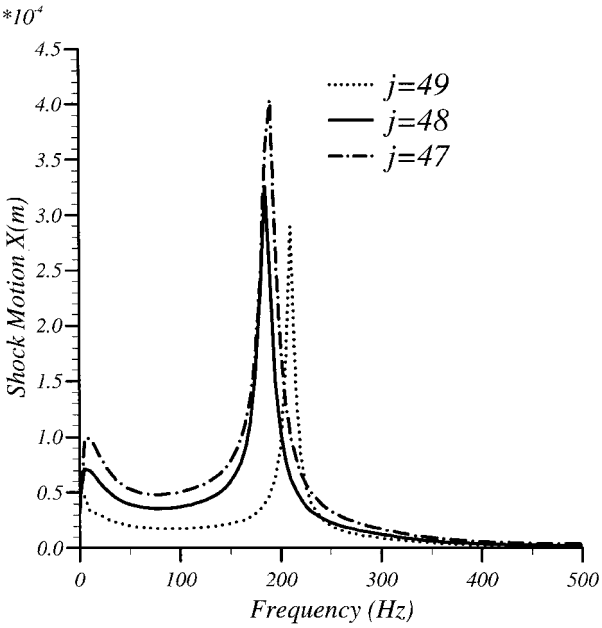

Fig. 9 *y*-dependence of shock motion spectrum.

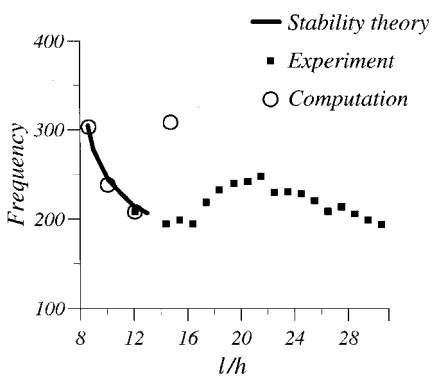

Fig. 10 Frequency vs diffuser length.

$l/h = 13$, the one-dimensional stability theory seems to be in good agreement with the experimental and numerical results. The four points with the label *computation* have been extracted from Fig. 3 (Ref. 3).

Evolution of ω_i with the Frequency

The main objective of a linear stability analysis is to determine if the basic flow is stable with respect to infinitesimal perturbations. This stability is characterized by the sign of the temporal amplification growth rate ω_i. Figure 11 shows the evolution of the temporal amplification coefficient ω_i; it is always negative whatever the frequency is. Therefore, according to the stability definition, the mean flow is stable. Thus if the mean flow could be strictly unperturbed (at the exit section by some pressure fluctuations), no shock oscillation and no perturbation in the downstream zone could be observed. This could be verified experimentally by adding a second throat close to the exit section to eliminate any downstream excitation.

Pressure Fluctuation

This section is devoted to the comparison between the experimental results of Sajben et al.[1] and the temporal stability results for the amplitude and the phase of the pressure fluctuation. The results are illustrated in Figs. 12 and 13. A difference is observed, mainly close to the shock. However, it is important to note that the amplitude for the theoretical curve in Fig. 12 corresponds to the single frequency $f = 200$ Hz, whereas the experimental amplitude covers a large frequency band.

On the other hand, concerning the phase variation (Fig. 13), there is a good agreement between stability and experimental results even if the theoretical results only concern one frequency ($f = 200$ Hz).

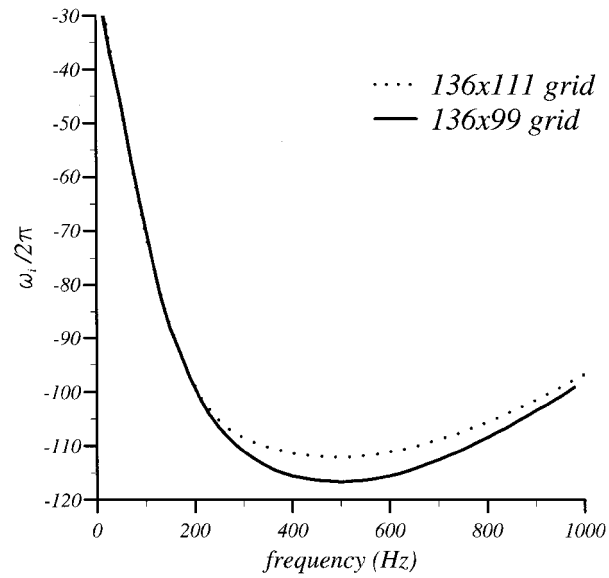

Fig. 11 Variation of ω_i.

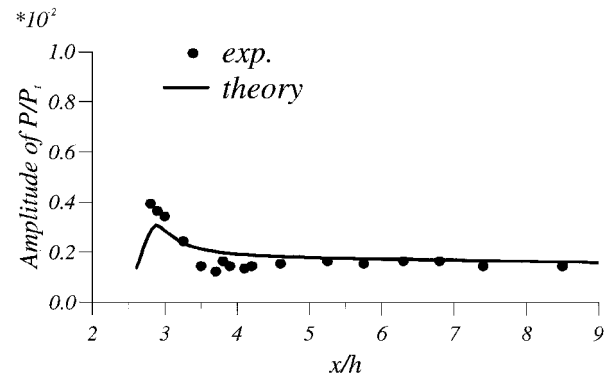

Fig. 12 Amplitude of fluctuating pressure.

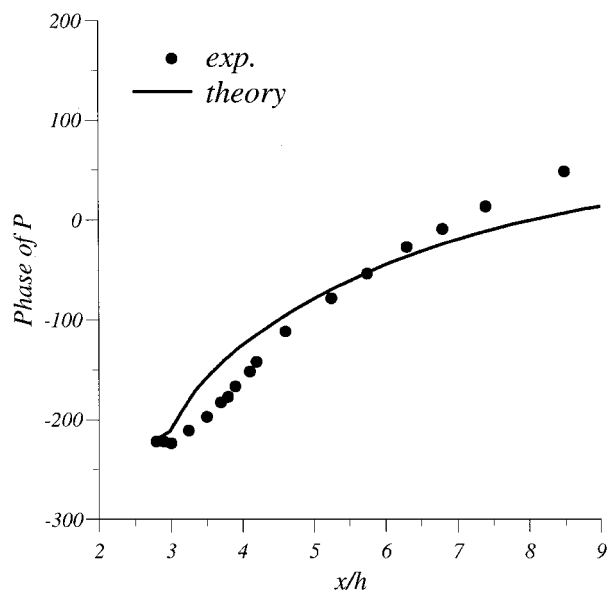

Fig. 13 Phase of the fluctuating pressure.

V. Conclusions

The goal of this paper is to present new approaches based on the small perturbation technique to explain and to predict the self-sustained shock oscillations observed in many diffusers: a 1*D* linear stability theory. In Sajben et al.'s[1] diffuser the mean flow in the core region can be considered as a quasi-one-dimensional flow. Then an appropriate stability analysis has been developed to try to understand and to predict the self-sustained oscillations origin. The comparisons between experimental data, numerical simulations, and linear theory

have shown that the latter can provide the frequency of the shock oscillations. Finally, this study can give some new insight into the physical origin of the observed self-excited shock oscillations. Indeed, this analysis can show that at least in some cases self-sustained shock oscillations can be predicted with an inviscid linear stability theory but with a mean flow computed with Navier–Stokes equations. The agreement between this theory and the experiment may suggest that the transverse waves carried by the boundary layer, in this case, are not the main mechanism to explain the observed self-sustained oscillations in transonic diffuser flow.

Appendix: Stability Calculations

To simplify the notations, the following quantities $\tilde{\omega}$ and Ω are introduced:

$$\tilde{\omega} = \omega - k\bar{V}, \qquad \Omega = \sqrt{k^2(\bar{a}^2 - \bar{U}^2) - \tilde{\omega}^2}$$

The eigenvalues of $\boldsymbol{C}^{-1}\boldsymbol{B}$ are

$$l_1 = \frac{-i\tilde{\omega}\bar{U} + \bar{a}\Omega}{\bar{a}^2 - \bar{U}^2}, \qquad l_2 = \frac{-i\tilde{\omega}\bar{U} - \bar{a}\Omega}{\bar{a}^2 - \bar{U}^2}, \qquad l_3 = l_4 = \frac{i\tilde{\omega}}{\bar{U}} \tag{A1}$$

and the eigenvectors of these eigenvalues are

$$\boldsymbol{V}_1 = \begin{bmatrix} (1/C_p k)(i\bar{U}l_1 + \tilde{\omega}) \\ (\bar{\rho}/k\bar{a})(i\bar{U}l_1 + \tilde{\omega}) \\ -(1/k\bar{U})i\bar{U}l_1 \\ 1 \end{bmatrix}, \qquad \boldsymbol{V}_2 = \begin{bmatrix} (1/C_p k)(i\bar{U}l_2 + \tilde{\omega}) \\ (\bar{\rho}/k\bar{a})(i\bar{U}l_2 + \tilde{\omega}) \\ -(1/k\bar{U})i\bar{U}l_2 \\ 1 \end{bmatrix} \tag{A2}$$

$$\boldsymbol{V}_3 = \begin{bmatrix} 1 \\ -\bar{\rho}/\bar{T} \\ 0 \\ 0 \end{bmatrix}, \qquad \boldsymbol{V}_4 = \begin{bmatrix} 0 \\ 0 \\ 1 \\ -\tilde{\omega}/k\bar{U} \end{bmatrix}$$

The matrix expressions of the differential system are

$$\boldsymbol{C} = \begin{bmatrix} 0 & \bar{U} & \bar{\rho} & 0 \\ r\bar{\rho} & r\bar{T} & \bar{\rho}\bar{U} & 0 \\ 0 & 0 & 0 & \bar{\rho}\bar{U} \\ C_p\bar{U}\bar{\rho} & 0 & \bar{\rho}\bar{U}^2 & \bar{\rho}\bar{U}\bar{V} \end{bmatrix} \tag{A3}$$

$$\boldsymbol{B} = \begin{bmatrix} 0 & a_{12} & -(\partial\bar{\rho}/\partial x) & -iky\bar{\rho} \\ -r(\partial\bar{\rho}/\partial x) & a_{22} & \bar{\rho}a_{12} & 0 \\ -irk\bar{\rho} & a_{32} & -\bar{\rho}(\partial\bar{V}/\partial x) & i\bar{\rho}\tilde{\omega} \\ i(\tilde{\omega}C_p - r\omega)\bar{\rho} & -i\tilde{\omega}r\bar{T} & \bar{\rho}\bar{u}a_{12} & a_{44} \end{bmatrix} \tag{A4}$$

with

$$a_{12} = i\tilde{\omega} - \frac{\partial\bar{U}}{\partial x}, \qquad a_{22} = -\bar{U}\frac{\partial\bar{U}}{\partial x} - r\frac{\partial\bar{T}}{\partial x}$$

$$a_{32} = -\bar{U}\frac{\partial\bar{V}}{\partial x} - irk\bar{T}, \qquad a_{44} = i\tilde{\omega}\bar{\rho}\bar{V} - \bar{\rho}\bar{U}\frac{\partial\bar{V}}{\partial x}$$

The vector and matrix expressions of algebraic system (18) are

$$\boldsymbol{A} = \begin{bmatrix} 0 & \bar{U}_1 & \bar{\rho}_1 & 0 \\ r\bar{\rho}_1 & \bar{U}_1 + r\bar{T}_1 & 2\bar{\rho}_1\bar{U}_1 & 0 \\ C_p & 0 & \bar{U}_1 & 0 \\ 0 & 0 & 0 & 1 \end{bmatrix} \tag{A5}$$

$\boldsymbol{\xi} = \boldsymbol{\xi}_0 - \boldsymbol{\xi}_1$ with

$$\boldsymbol{\xi}_i = \begin{bmatrix} \dfrac{\partial}{\partial x}(\bar{\rho}_i\bar{U}_i) + i(\omega - k\bar{V}_i)\bar{\rho}_i \\ \dfrac{\partial}{\partial x}\left(\bar{p}_i + \bar{\rho}_i\bar{U}_i^2\right) + 2i(\omega - k\bar{V}_i)\bar{\rho}_i\bar{U}_i \\ \dfrac{\partial}{\partial x}\left(C_p\bar{T}_i + \dfrac{1}{2}\bar{U}_i^2\right) + i(\omega - k\bar{V}_i)\bar{U}_i \\ \dfrac{\partial\bar{V}_i}{\partial x} + ik\bar{U}_i \end{bmatrix} \tag{A6}$$

Acknowledgments

This study has been carried out under Contract 93/CNES/3040 granted by the French Centre National d'Etudes Spatiales. The mean flow has been computed by R. Hallard (ONERA).

References

[1]Sajben, M., Bogar, T. J., and Kroutil, J. C., "Characteristic Frequency and Length Scales in Transonic Diffuser Flow Oscillations," AIAA Paper 81-1291, June 1981.

[2]Liou, M. S., Coakley, T. J., and Bergmann, M. Y., "Numerical Simulation of Transonic Flows in Diffusers," AIAA Paper 81-1240, June 1981.

[3]Hsieh, T., and Coakley, T. J., "Downstream Boundary Effects on the Frequency of Self-Excited Oscillations in Diffuser Flows," AIAA Paper 87-0161, Jan. 1987.

[4]Bogar, T. J., Sajben, M., and Kroutil, J. C., "Characteristic Frequencies of Transonic Diffuser Flow Oscillations," *AIAA Journal*, Vol. 21, No. 9, pp. 1983, 1232–1240.

[5]Sajben, M., and Bogar, T. J., "Unsteady Transonic Flow in a Two-Dimensional Diffuser: Interpretation of Experimental Results," McDonnell Douglas Corp., Rept. MDC Q0779, Air Force Office of Scientific Research, March 1982.

[6]Liou, M. S., and Coakley, T. J., "Numerical Simulation of Unsteady Transonic Flows in Diffusers," AIAA Paper 82-1000, June 1982.

[7]Casalis, G., Hallard, R., Jouet, C., and Robinet, J.-C., "Calcul des Caractéristiques Stationnaires et Instationnaires d'un Écoulement Décollé dans un Tuyère, cas Bidimensionnel," ONERA, TN RT 93/3040, Toulouse, France, Sept. 1996.

[8]Cambier, L., Darracq, D., Gazaix, M., Gullien, Ph., Jouet, Ch., and Le Toullec, L., "Améliorations Récentes du code D'écoulements Compressibles FLU3M," *Progress and Challenges in CFD Methods and Algorithms*, CP-578, AGARD, April 1996.

[9]Gleize, V., and Jouet, C., "Introduction de Modèles de Turbulence dans les Codes Navier–Stokes: Applications à des Écoulement Bidimensionnels," *30ième Colloque d'Aérodynamique Appliquée*, Association Aéronautique et Astronautique de France, Oct. 1995.

[10]Kantrowitz, A., "The Formation and Stability of Normal Shock Waves in Channel Flows," NACA TN-1225, March 1947.

[11]Casalis, G., and Robinet, J.-Ch., "Linear Stability Analysis in Transonic Diffuser Flow," *Aerospace Science and Technology*, Vol. 1, No. 1, 1998, pp. 37–47.

[12]Culick, F. E. C., and Rogers, T., "The Response of Normal Shocks in Diffusers," *AIAA Journal*, Vol. 21, No. 10, 1983, pp. 1382–1390.

[13]Robinet, J.-C., and Casalis, G., "Analyse de Stabilité Linéaire Bidimensionnelle d'un Écoulement de Tuyère Présentant un Choc," ONERA, Dept. of Modelling Aerodynamics and Energetics, TN RT 98/5605.98, Toulouse, France, July 1997.

K. Kailasanath
Associate Editor